INSTITUTE OF PHYSICS PUBLISHING JOURNAL OF OPTICS B: QUANTUM AND SEMICLASSICAL OPTICS

J. Opt. B: Quantum Semiclass. Opt. **6** (2004) S715–S721 PII: S1464-4266(04)72016-9

Fluorescence squeezing spectra near a photonic bandgap

Ray-Kuang Lee[1,2] **and Yinchieh Lai**[1,3]

[1] Institute of Electro-Optical Engineering, National Chiao-Tung University, Hsinchu, Taiwan, R.O.C. 300
[2] National Center for High-Performance Computing, Hsinchu, Taiwan, R.O.C. 300

E-mail: yclai@mail.nctu.edu.tw

Received 15 November 2003, accepted for publication 16 February 2004
Published 27 July 2004
Online at stacks.iop.org/JOptB/6/S715
doi:10.1088/1464-4266/6/8/014

Abstract
The fluorescence intensity and quadrature spectra from a two-level atom embedded in a photonic bandgap crystal and resonantly driven by a classical pump light are calculated. The non-Markovian nature of the problem caused by the non-uniform distribution of the photonic density of states is handled by linearizing the generalized optical Bloch equations with the Liouville operator expansion. Unlike the case in free space, we find that the bandgap effects will not only modify the fluorescence spectral shape but also cause squeezing in the in-phase quadrature spectra.

Keywords: fluorescence spectra, photonic bandgap materials, cavity quantum electrodynamics, squeezing spectra

(Some figures in this article are in colour only in the electronic version)

1. Introduction

The study of fluorescence spectra from two-level atoms has been a central topic in quantum optics since the beginning of quantum mechanics in the 1930s. From the view point of light scattering, both elastic Rayleigh scattering and inelastic Raman scattering processes are involved [1] and thus the fluorescence spectra will have a triplet shape as first calculated by Mollow [2]. Theoretical calculations of the fluorescence spectra have been explored [3, 4] and also verified in experiments [5]. The squeezing phenomena in the phase-dependent fluorescence spectra of the quadrature field components were first predicted by Walls and Zoller [6] and Mandel [7]. It has been theoretically shown that the squeezing can be found in the out-of-phase quadrature component spectra under the condition that $\Omega^2 < 4\Gamma^2$ [8, 9], where Ω is the Rabi frequency and Γ is the atomic decay rate. Squeezed fluorescence spectra have also been experimentally observed in an experiment using ^{174}Yb atoms [10].

In recent years the atom–photon interaction in photonic bandgap materials [11, 12] has been found to exhibit many interesting new phenomena such as photon–atom bound states [13], spectral splitting [14], quantum interference dark line effect [15], phase control of spontaneous emission [16], transparency near band edge [17], and single-atom switching [18]. From the Aulter–Townes spectra for atoms coupled to a photonic bandgap structure [14] (or equivalently a frequency-dependent photon density of states [19]), the modification of the spontaneous emission caused by the environment (the Purcell effect [20]) can actually be verified. However, all of the above studies only focused on the transient behaviour of the atom–photon interactions and to the best of our knowledge there is still no theoretical treatment on calculating the steady-state fluorescence spectra in photonic bandgap crystals.

In the theoretical studies of fluorescence spectra for the free space case, the Markovian approximation is usually used to describe the statistical properties of the optical noises. This is a good assumption for the free space case but is not applicable for the case of photonic bandgap crystals. This is because in a photonic bandgap crystal, the propagation of light is prohibited within a certain range of wavelengths (the bandgap) due to the lack of available photon states. Because of the bandgap effects, the distributions of the photonic density of states (DOS) are typically highly non-uniform near the bandedge. Such a property has prohibited the direct applicability of the Markovian approximation to simplify the derivation for the problem we are going to consider.

[3] Author to whom any correspondence should be addressed.

The aim of this paper is to investigate the properties of the steady state resonance fluorescence emitted by a two-level atom embedded in a photonic bandgap crystal and driven by a classical pumping light. We treat the photon states in the photonic crystal as the background reservoir and obtain a set of generalized Bloch equations for the atomic operators by eliminating the reservoir field operators. The non-uniform DOS distributions near the bandedge are modelled by the three-dimensional anisotropic dispersion relation [21] and the Liouville operator expansion is used to reduce the two-time atomic operator products into equal-time atomic operator products. In this way the nonlinear generalized Bloch equations are reduced into a set of linear equations with memory function terms caused by the atom–reservoir interaction. This set of linear equations can then be easily solved in the frequency domain, and the resonance fluorescence spectra can be directly obtained from the correlation functions of the atomic operators in the frequency domain without applying the quantum regression theorem. After performing a numerical calculation, we find that the spectral shape of the fluorescence intensity spectra will vary with the wavelength offset between the atomic transition wavelength and the bandedge. More interestingly, squeezing phenomena are found to be present in the in-phase quadrature spectra instead of the out-of-phase quadrature spectra.

The paper is organized as follows. In section 2 we derive the generalized optical Bloch equations with noise operators caused by the surrounding photonic reservoir. In section 3 we use the anisotropic dispersion relation for modelling the photon DOS of the three-dimensional photonic bandgap structure, and based on this model the fluorescence spectra are calculated. The squeezing in the phase-dependent fluorescence spectra of a two-level atom both in free space and near a photonic bandgap is shown in section 4. Finally, a brief conclusion is given in section 5.

2. Theoretical model

To begin the derivation, the Hamiltonian for the system to be considered can be written as

$$H = \frac{\hbar}{2}\omega_a\sigma_z + \hbar\sum_k \omega_k a_k^\dagger a_k + \frac{\Omega}{2}\hbar(\sigma_- e^{i\omega_L t} + \sigma_+ e^{-i\omega_L t}) + \hbar\sum_k (g_k\sigma_+ a_k + g_k^* a_k^\dagger \sigma_-). \quad (1)$$

Here the transition frequency of the atom and the frequency of the pumping light are denoted by ω_a and ω_L respectively, $a_k^\dagger$ and a_k are the creation and annihilation operators of the photon states in the photonic bandgap crystals, Ω is the Rabi-flopping frequency of the atom under the external pumping light and it also represents the relative magnitude of the pumping light, $\sigma_z \equiv (|2\rangle\langle 2| - |1\rangle\langle 1|)$, $\sigma_+ \equiv |2\rangle\langle 1| = \sigma_-^\dagger$ are the usual Pauli matrices for the two-level atom, and g_k is the atom–field coupling constant. We have used the index k to label different photon states, and the coupling constant g_k can be expressed as

$$g_k(\hat{\mathbf{d}}, \vec{r}_0) \equiv g_k = |d|\omega_a\sqrt{\frac{1}{2\hbar\epsilon_0\omega_k V}}\hat{\mathbf{d}}\cdot\mathbf{E}_k^*(\vec{r}_0). \quad (2)$$

We have used the notations $|d|$ for the magnitude of the atomic dipole moment, $\hat{\mathbf{d}}$ for the unit vector along the direction of the dipole moment, V for the volume of the quantization space, and ϵ_0 for the Coulomb constant.

Starting from the Hamiltonian, we treat the photon field operators as the background reservoir and eliminate their corresponding equations to obtain the following set of generalized Bloch equations.

$$\dot\sigma_-(t) = i\frac{\Omega}{2}\sigma_z(t)e^{-i\Delta t} + \int_{-\infty}^{t} dt'\, G(t-t')\sigma_z(t)\sigma_-(t') + n_-(t) \quad (3)$$

$$\dot\sigma_+(t) = -i\frac{\Omega}{2}\sigma_z(t)e^{i\Delta t} + \int_{-\infty}^{t} dt'\, G_c(t-t')\sigma_+(t')\sigma_z(t) + n_+(t) \quad (4)$$

$$\dot\sigma_z(t) = i\Omega(\sigma_-(t)e^{i\Delta t} - \sigma_+(t)e^{-i\Delta t} + n_z(t) - 2\int_{-\infty}^{t} dt'\,[G(t-t')\sigma_+(t)\sigma_-(t') + G_c(t-t')\sigma_+(t')\sigma_-(t)]. \quad (5)$$

Here $\Delta \equiv \omega_L - \omega_a$ and $\Delta_k \equiv \omega_a - \omega_k$. The two functions $G(\tau)$ and $G_c(\tau)$ are the memory functions of the system caused by the atom–reservoir interaction and they are defined as $G(\tau) \equiv \sum_k |g_k|^2 e^{i\Delta_k\tau}\Theta(\tau)$, and $G_c(\tau) \equiv \sum_k |g_k|^2 e^{-i\Delta_k\tau}\Theta(\tau)$. Here $\Theta(\tau)$ is the Heaviside step function. The three noise operators $n_-(t)$, $n_+(t)$, and $n_z(t)$ originate from the original photon filed operator before interaction and are expressed as follows:

$$n_-(t) = i\sum_k g_k e^{i\Delta_k t}\sigma_z(t)a_k(-\infty) \quad (6)$$

$$n_+(t) = -i\sum_k g_k^* e^{-i\Delta_k t}a_k^\dagger(-\infty)\sigma_z(t) \quad (7)$$

$$n_z(t) = -2i\sum_k g_k e^{i\Delta_k t}\sigma_+(t)a_k(-\infty) + 2i\sum_k g_k^* e^{-i\Delta_k t}a_k^\dagger(-\infty)\sigma_-(t). \quad (8)$$

Supposing that the reservoir is in thermal equilibrium, then the mean and the correlation functions of the reservoir field operators before interaction will be

$$\langle a_k(-\infty)\rangle_R = \langle a_k^\dagger(-\infty)\rangle_R = 0 \quad (9)$$

$$\langle a_k(-\infty)a_{k'}(-\infty)\rangle_R = 0 \quad (10)$$

$$\langle a_k^\dagger(-\infty)a_{k'}^\dagger(-\infty)\rangle_R = 0 \quad (11)$$

$$\langle a_k^\dagger(-\infty)a_{k'}(-\infty)\rangle_R = \bar n_k\delta_{kk'} \quad (12)$$

$$\langle a_k(-\infty)a_{k'}^\dagger(-\infty)\rangle_R = (\bar n_k + 1)\delta_{kk'}. \quad (13)$$

Here $\bar n_k$ is the mean quantum numbers of the reservoir modes under thermal equilibrium. Using the statistical characteristics of the reservoir field operators, it can easily be shown that the three noise operators $n_-(t)$, $n_+(t)$, and $n_z(t)$ are zero mean with their correlation functions given below:

$$\langle n_-(t)\rangle_R = \langle n_+(t)\rangle_R = \langle n_z(t)\rangle_R = 0$$

$$\langle n_-(t)n_-(t')\rangle_R = \langle n_+(t)n_+(t')\rangle_R = 0$$

$$\langle n_-(t)n_+(t')\rangle_R = \sum_k |g_k|^2(\bar n_k + 1)e^{i\Delta_k(t-t')}\langle\sigma_z(t)\sigma_z(t')\rangle$$

$$\langle n_+(t)n_-(t')\rangle_R = \sum_k |g_k|^2\bar n_k e^{-i\Delta_k(t-t')}\langle\sigma_z(t)\sigma_z(t')\rangle$$

$$\langle n_z(t)n_z(t')\rangle_R = 4\sum_k |g_k|^2[(\bar n_k + 1)e^{i\Delta_k(t-t')}\langle\sigma_+(t)\sigma_-(t')\rangle + \bar n_k e^{-i\Delta_k(t-t')}\langle\sigma_-(t)\sigma_+(t')\rangle].$$

Since in general the correlation functions of these noise operators are not delta-correlated with time (non-Markovian), we cannot directly use the Born–Markovian approximation to solve the problem. One can see that the correlation functions depend not only on the photon density of states, but also on the correlations of the atomic operators. Equations (3)–(5) are called the generalized optical Bloch equations and will serve as the starting point for our further derivation.

3. Fluorescence spectra

To actually evaluate the memory functions as well as the correlation functions of the noise operators, one needs to know the spectral distribution of the photonic density of states. Although in general the DOS of photonic bandgap crystals is very complicated and also varies with the geometrical structure and the dielectric constants of the material, it is still possible to approximately model the DOS near the bandedge with a simple formula. According to the results from the full vectorial numerical calculation, the DOS near the bandgap for three-dimensional photonic crystals increases from zero and behaves more like the anisotropic model proposed in the literature [21]. To be more specific, for a three-dimensional photonic bandgap crystal, if the wavevector that corresponds to the bandedge is $\mathbf{k}_0^i$, then the dispersion relation in the anisotropic model is described by the following form: $\omega_k = \omega_c + A|\mathbf{k} - \mathbf{k}_0^i|^2$, where A is a model dependent constant and ω_c is the bandedge frequency. Based on this dispersion relation, the corresponding DOS is given by $D(\omega) = \frac{1}{A^{3/2}}\sqrt{\omega - \omega_c}\Theta(\omega - \omega_c)$. The memory functions under this anisotropic model also can be derived as

$$\tilde{G}(\omega) = \beta^{3/2}\frac{-\mathrm{i}}{\sqrt{\omega_c} + \sqrt{\omega_c - \omega_a - \omega}} \tag{14}$$

$$\tilde{G}_c(\omega) = \beta^{3/2}\frac{\mathrm{i}}{\sqrt{\omega_c} + \sqrt{\omega_c - \omega_a + \omega}} \tag{15}$$

where $\beta^{3/2} = \frac{\omega_a^2 d^2}{6\hbar\epsilon_0\pi A^{3/2}}\eta$, and we have used the space average coupling strength $\eta \equiv \frac{3}{8\pi}\int \mathrm{d}\Omega\,|\hat{\mathbf{d}}\cdot\mathbf{E}|^2$ in the derivation.

From figure 1, the spectrum of the memory function $G(\omega)$ is non-uniform and asymmetric as we expect. When the frequency is far from the bandedge frequency ω_c, the memory function is a pure real function which corresponds to the decay rate of the atom. When the frequency is below the bandedge frequency, the memory function becomes pure imaginary, indicating the inhibition of the spontaneous emission inside the bandgap. And in between the memory function is a complex function, of which the real part is related to the decay process and the imaginary part is related to the oscillation process. The spectrum for another memory function $G_c(\omega)$ is also similar. All the frequency parameters used in the calculation are expressed in terms of the normalized frequency unit β defined above, and are labelled in the figure. The normalized frequency unit β corresponds to but is not exactly equal to the decay rate of the excited atom, Γ, in the case of free space. In fact, if we define the memory functions of free space as delta-functions, i.e. $\sum_k |g_k|^2 \mathrm{e}^{\pm\mathrm{i}\Delta_k t} = \Gamma\delta(t)$, then the relation between the normalized frequency of the anisotropic model near the photonic bandgap and the free space decay rate can be estimated from equation (14) with $\omega_c \ll \omega_a$.

$$\Gamma \approx \beta^{3/2}/\sqrt{\omega_a}. \tag{16}$$

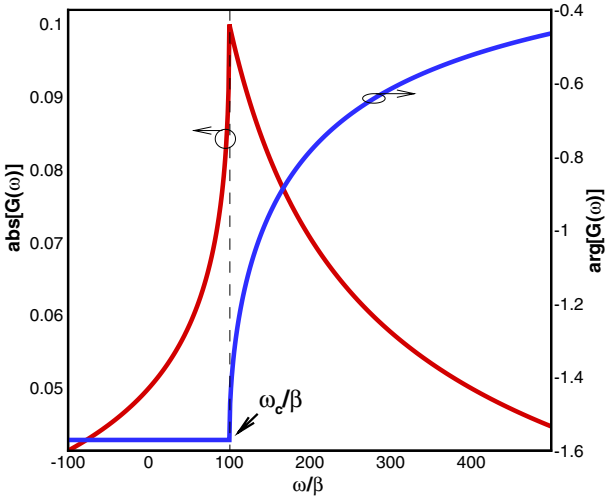

Figure 1. Amplitude and phase spectra of the memory function $G(\omega)$ with bandedge frequency $\omega_c = 100\beta$. The memory function is non-uniform around the bandedge and becomes pure imaginary inside the bandgap.

From this estimation, the value of the normalized frequency β will be in the range of $0.01\Gamma < \beta < 100\Gamma$ [18].

The generalized Bloch equations are a set of nonlinear operator equations and they cannot be solved easily. To overcome this difficulty, we introduce the following Liouville operator expansion:

$$\begin{aligned}\sigma_{ij}(t) &= \mathrm{e}^{-\mathrm{i}\mathcal{L}(t-t')}\sigma_{ij}(t') \\ &= \sum_{n=0}^{\infty}\frac{[-\mathrm{i}(t-t')]^n}{n!}\mathcal{L}^n\sigma_{ij}(t').\end{aligned} \tag{17}$$

Here the Liouville superoperator $\mathcal{L}$ is defined as $\mathcal{L}^n\sigma_{ij}(t') = \hbar^n[[\cdots[\sigma_{ij}(t'), H], H], \ldots, H]$. If the atom we consider is with a longer lifetime and the pumping is not extremely high, which is the usual case in the optical domain, then the timescale of the atomic evolution will be longer than the timescale of the memory functions. Therefore under such assumptions it should be legitimate to simply apply the zeroth-order perturbation term (zeroth-order Born approximation) [18]. This is equivalent to using the equal-time operator products to replace the two-time operator products. With these approximations and by using the identities of Pauli matrices, the generalized optical Bloch equations can be reduced into the following form:

$$\dot{\sigma}_-(t) = \mathrm{i}\frac{\Omega}{2}\sigma_z(t)\mathrm{e}^{-\mathrm{i}\Delta t} - \int_{-\infty}^{t}\mathrm{d}t'\,G(t-t')\sigma_-(t') + n_-(t) \tag{18}$$

$$\dot{\sigma}_+(t) = -\mathrm{i}\frac{\Omega}{2}\sigma_z(t)\mathrm{e}^{\mathrm{i}\Delta t} - \int_{-\infty}^{t}\mathrm{d}t'\,G_c(t-t')\sigma_+(t') + n_+(t) \tag{19}$$

$$\begin{aligned}\dot{\sigma}_z(t) &= \mathrm{i}\Omega(\sigma_-(t)\mathrm{e}^{\mathrm{i}\Delta t} - \sigma_+(t)\mathrm{e}^{-\mathrm{i}\Delta t}) \\ &\quad - \int_{-\infty}^{t}\mathrm{d}t'\,[G(t-t') + G_c(t-t')](1+\sigma_z(t')) + n_z(t).\end{aligned} \tag{20}$$

The approximation we have used should be valid as long as the timescale of the memory function is still much shorter than the timescale of the atomic response (i.e., the

inverse of the Rabi frequency and the decay rate). It can be easily checked that the full-width-half-maximum (FWHM) bandwidth of the memory functions in equations (14) and (15) are $4\omega_c$. For a bandgap in the optical domain, the order of ω_c is about 10^{14}–10^{15} Hz, and the typical lifetime of the atom is from 10^{-3} to 10^{-9} s, which is much longer than the response time of the memory functions. However, in contrast to the Markovian approximation, we do not approximate the memory function by a δ-function, but instead still keep its finite response characteristics in order to include the effects due to the non-uniform density of states near the bandedge. Although such a simple approximation includes only one portion of the non-Markovian nature of the problem, it should still be quite valid for the fluorescence spectrum calculation considered in the present work, since here the memory function timescale is typically much shorter than the atomic response timescale. We have also checked the validity of the zeroth-order approximation used here by carrying out the derivation in which the first-order expansion term is also included (first-order Born approximation) [22]. In the numerical examples to be presented later we choose $\omega_c = 100\beta$ and $\Omega = 0.25\beta$ to illustrate the fluorescence spectra clearly by setting the Rabi frequency to be somewhat larger than the atomic decay rate, but still much smaller than the inverse of the response time of the memory functions. The zeroth-order Liouville operator expansion we have used should be quite accurate within such a parameter range. The results for higher ω_c/β ratios exhibit qualitatively similar behaviour.

Theoretically the fluorescence spectrum can be calculated by taking the Fourier transform of the first-order correlation function of the atomic dipole moment operator. By using a Fourier transform, we can directly solve these modified optical Bloch equations as follows:

$$\overline{\overline{\mathcal{M}}}(\omega)\cdot\vec{\mathcal{X}}(\omega)=\vec{\mathcal{X}}_0(\omega) \tag{21}$$

where

$$\overline{\overline{\mathcal{M}}}(\omega)=\begin{pmatrix} -\mathrm{i}(\omega+\Delta)+\tilde{G}(\omega) & 0 & -\mathrm{i}\frac{\Omega}{2} \\ 0 & -\mathrm{i}(\omega-\Delta)+\tilde{G}_c(\omega) & \mathrm{i}\frac{\Omega}{2} \\ -\mathrm{i}\Omega & \mathrm{i}\Omega & -\mathrm{i}\omega+\tilde{G}(\omega)+\tilde{G}_c(\omega) \end{pmatrix}$$

$$\vec{\mathcal{X}}(\omega)=\begin{pmatrix} \tilde{\sigma}_-(\omega+\Delta) \\ \tilde{\sigma}_+(\omega-\Delta) \\ \tilde{\sigma}_z(\omega) \end{pmatrix},\qquad \text{and}$$

$$\vec{\mathcal{X}}_0(\omega)=\begin{pmatrix} \tilde{n}_-(\omega+\Delta) \\ \tilde{n}_+(\omega-\Delta) \\ -2\pi[\tilde{G}(\omega)+\tilde{G}_c(\omega)]\delta(\omega)+\tilde{n}_z(\omega) \end{pmatrix}$$

and $\tilde{n}_-(\omega)$, $\tilde{n}_+(\omega)$, $\tilde{n}_z(\omega)$, $\tilde{G}(\omega)$, and $\tilde{G}_c(\omega)$ are Fourier transforms of $n_-(t), n_+(t), n_z(t), G(t)$, and $G_c(t)$, respectively. The solutions of equation (21) are

$$\begin{aligned}\tilde{\sigma}_-(\omega+\Delta)&=\{(2g_\omega h_\omega+\Omega^2)\tilde{n'}_{-\omega}+\Omega^2\tilde{n'}_{+\omega}\\&\quad+\mathrm{i}g_\omega\Omega\tilde{n}_z(\omega)-\mathrm{i}2\pi g_\omega\Omega\tilde{G'}_\omega\delta(\omega)\}\\&\quad\times\{\Omega^2(f_\omega+g_\omega)+2f_\omega g_\omega h_\omega\}^{-1}\end{aligned} \tag{22}$$

$$\begin{aligned}\tilde{\sigma}_+(\omega-\Delta)&=\{\Omega^2\tilde{n'}_{-\omega}+(2f_\omega h_\omega+\Omega^2)\tilde{n'}_{+\omega}\\&\quad-\mathrm{i}f_\omega\Omega\tilde{n}_z(\omega)+\mathrm{i}2\pi f_\omega\Omega\tilde{G'}_\omega\delta(\omega)\}\\&\quad\times\{\Omega^2(f_\omega+g_\omega)+2f_\omega g_\omega h_\omega\}^{-1}\end{aligned} \tag{23}$$

$$\begin{aligned}\tilde{\sigma}_z(\omega)&=\{2\mathrm{i}g_\omega\Omega\tilde{n'}_{-\omega}-2\mathrm{i}f_\omega\Omega\tilde{n'}_{+\omega}\\&\quad+2f_\omega g_\omega\tilde{n}_z(\omega)-4\pi f_\omega g_\omega\tilde{G'}_\omega\delta(\omega)\}\\&\quad\times\{\Omega^2(f_\omega+g_\omega)+2f_\omega g_\omega h_\omega\}^{-1}.\end{aligned} \tag{24}$$

Here we have used the following shorthand notations:

$$f_\omega=f(\omega)\equiv-\mathrm{i}\omega-\mathrm{i}\Delta+\tilde{G}(\omega)$$

$$g_\omega=g(\omega)\equiv-\mathrm{i}\omega+\mathrm{i}\Delta+\tilde{G}_c(\omega)$$

$$h_\omega=h(\omega)\equiv-\mathrm{i}\omega+\tilde{G}(\omega)+\tilde{G}_c(\omega)$$

$$\tilde{n'}_{\pm\omega}=\tilde{n'}_\pm(\omega)\equiv\tilde{n}_\pm(\omega\mp\Delta)$$

$$\tilde{G'}_\omega=\tilde{G'}(\omega)\equiv\tilde{G}(\omega)+\tilde{G}_c(\omega).$$

Because the two-time correlation function of the atomic dipole is proportional to the first-order coherence function $g^{(1)}(\tau)$ [23] of the radiated photon field and the fluorescence spectrum can be obtained by taking the Fourier transform of the first-order coherence function, one has

$$S(\omega)=\int_{-\infty}^{\infty}\mathrm{d}\tau\, g^{(1)}(\tau)\mathrm{e}^{\mathrm{i}\omega\tau}\propto\langle\tilde{\sigma}_+(\omega)\tilde{\sigma}_-(-\omega)\rangle_R. \tag{25}$$

In this way the fluorescence spectrum can be easily determined after determining the noise correlation functions. By using the anisotropic model from equations (14), (15), the noise correlation functions near a photonic bandgap reservoir are given as

$$\langle\tilde{n}_-(\omega_1)\tilde{n}_+(-\omega_2)\rangle_R=\pi N(\omega_1)\Theta(\omega_1+\omega_a-\omega_c)\delta(\omega_1-\omega_2) \tag{26}$$

$$\begin{aligned}\langle\tilde{n}_z(\omega_1)\tilde{n}_z(-\omega_2)\rangle_R&=N(\omega_1)[4\pi\delta(\omega_1-\omega_2)\\&\quad+\langle\tilde{\sigma}_z(\omega_1-\omega_2)\rangle_R]\cdot\Theta(\omega_1+\omega_a-\omega_c)\end{aligned} \tag{27}$$

$$\langle\tilde{n}_z(\omega_1)\tilde{n}_-(-\omega_2)\rangle_R=0 \tag{28}$$

$$\begin{aligned}&\langle\tilde{n}_-(\omega_1)\tilde{n}_z(-\omega_2)\rangle_R\\&\quad=N(\omega_1)\langle\tilde{\sigma}_-(\omega_1-\omega_2)\rangle_R\Theta(\omega_1+\omega_a-\omega_c)\end{aligned} \tag{29}$$

$$\begin{aligned}&\langle\tilde{n}_z(\omega_1)\tilde{n}_+(-\omega_2)\rangle_R\\&\quad=N(\omega_1)\langle\tilde{\sigma}_+(\omega_1-\omega_2)\rangle_R\Theta(\omega_1+\omega_a-\omega_c)\end{aligned} \tag{30}$$

$$\langle\tilde{n}_+(\omega_1)\tilde{n}_z(-\omega_2)\rangle_R=0 \tag{31}$$

with

$$N(\omega)\equiv4\beta^{3/2}\frac{\sqrt{\omega_a+\omega-\omega_c}}{\omega_a+\omega}. \tag{32}$$

It can be easily seen from the above correlation functions that the statistics of the quantum noises of the photonic bandgap reservoir are not only colour noises but also exhibit bandgap behaviour.

Based on the above formula, in figure 2 we plot the resonance fluorescence spectra at a constant Rabi frequency when the atomic transition frequencies ω_a are far from (dashed curve) and near (solid curve) the bandedge frequency ω_c, respectively. The evolution of the resonance fluorescence spectra with different offsets between the transition frequency and the bandedge frequency is also plotted in figure 3. When the atomic transition frequency is far away from the bandedge ($\omega_a \gg \omega_c$), the normal resonance fluorescence spectrum of Mollow's triplets with three Lorentzian profiles is obtained just as expected [2]. The contribution from the elastic Rayleigh scattering in the centre part (which is a delta-function with zero detuning frequency) has been ignored and only the contribution from the inelastic Raman scattering (the three peaked profiles) are considered here. It can be noted that the separation of each

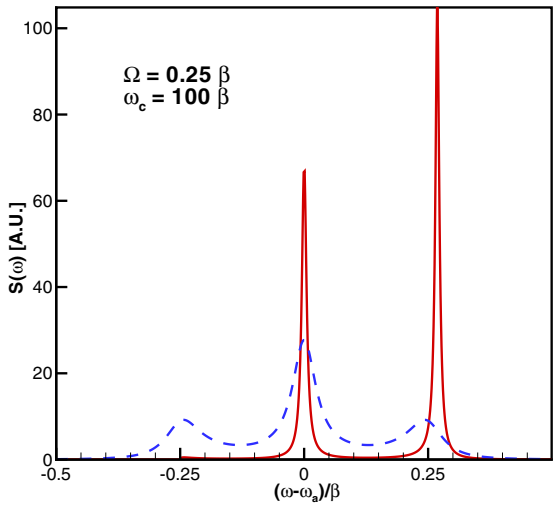

Figure 2. Comparison of resonance fluorescence spectra far from the bandedge (dashed curve, $\omega_a - \omega_c = 1000\beta$) and near the bandedge (solid curve $\omega_a - \omega_c = \Omega$); $\Omega = 0.25\beta$, $\omega_c = 100\beta$.

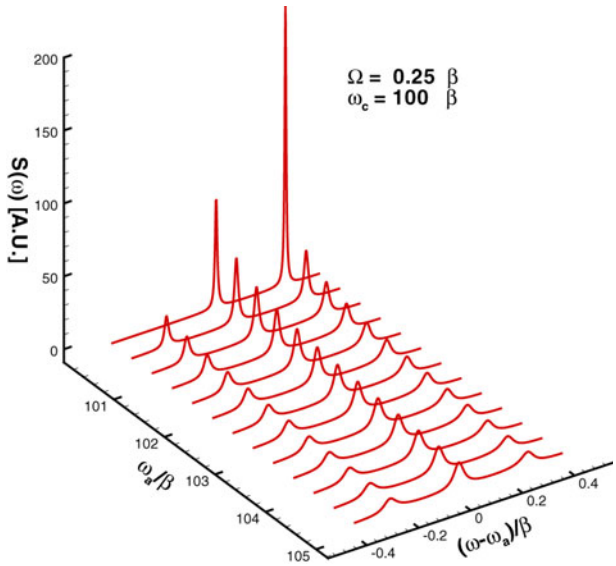

Figure 3. Evolution of the resonance fluorescence spectrum near the bandedge at constant Rabi frequency: $\Omega = 0.25\beta$, $\omega_c = 100\beta$.

adjacent peak is determined by the Rabi frequency as in the case of free space, and the linewidth of each peak is proportional to the decay rate of the atom. In the studied case we have set the Rabi frequency to be somewhat larger than the atomic decay rate so that the Mollow triplets are well separated.

When the atomic transition frequency moves towards the bandedge, the profiles due to incoherent scattering processes become increasingly sharp because there are successively fewer DOS available. The narrowing of the fluorescence spectra also indicates a smaller decay rate due to the forbidden effect of the bandgap. The profile in the lower frequency is not only suppressed but also becomes asymmetrical due to the existence of the bandgap. It should also be noted that the peak in the higher frequency is significantly enhanced, as can be clearly seen in the figure. Eventually the peak in the lower frequency will be totally suppressed when the atomic transition

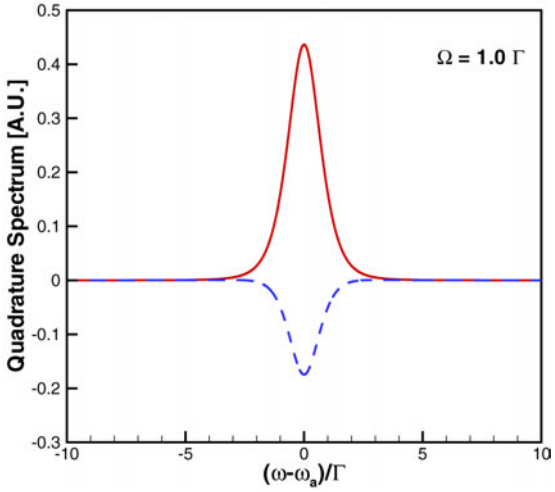

Figure 4. Resonance fluorescence quadrature spectra in free space. Solid curve: in-phase, $S_1(\omega)$; dashed curve: out-of-phase, $S_2(\omega)$ with $\Omega = 1.0\Gamma$, $\Gamma = 1.0$.

frequency moves more towards the bandedge. At this time the resonance fluorescence spectrum now only has two peaks.

4. Fluorescence squeezing spectra

The noise spectra of a two-level atom driven by a classical pumping light can also exhibit non-classical phenomena (squeezing spectra) if the phase-dependent fluorescence spectra are measured. To observe squeezing in the phase-dependent fluorescence spectra, one needs to calculate the fluorescence spectra for the quadrature field components. Theoretically the quadrature field operator in the θ phase angle is defined as

$$\hat{E}_\theta(t) = \mathrm{e}^{\mathrm{i}\theta}\hat{E}^{(+)}(t) + \mathrm{e}^{-\mathrm{i}\theta}\hat{E}^{(-)}(t). \tag{33}$$

The two cases corresponding to $\theta = 0$ and $\pi/2$ represent the in-phase and out-of-phase components of the electric field, respectively. The spectra for the quadrature fields can be obtained by calculating the following normal order variance:

$$\begin{aligned} S_\theta(\omega) &\equiv \langle \tilde{E}_\theta(\omega), \tilde{E}_\theta(-\omega)\rangle \\ &= \Gamma\tfrac{1}{4}[\langle\tilde{\sigma}_-(\omega)\tilde{\sigma}_-(-\omega)\rangle\mathrm{e}^{-2\mathrm{i}\theta} + \langle\tilde{\sigma}_+(\omega)\tilde{\sigma}_-(-\omega)\rangle \\ &\quad + \langle\tilde{\sigma}_+(-\omega)\tilde{\sigma}_-(\omega)\rangle + \langle\tilde{\sigma}_+(-\omega)\tilde{\sigma}_+(\omega)\rangle\mathrm{e}^{2\mathrm{i}\theta}] \end{aligned} \tag{34}$$

where the correlation functions have been renormalized with the total outgoing flux and Γ is the decay rate of the two-level atom [8, 9].

In the free space case, the in-phase quadrature $S_1(\omega)$ produces the central peak of the Mollow's triplet while the out-of-phase quadrature $S_2(\omega)$ produces the two side-peaks when the separation of the two sidebands is large. When the Rabi frequency is small (small driving field), $\Omega^2 < 4\Gamma^2$, squeezing can be observed in the out-of-phase quadrature spectra, as shown in figure 4. In the literature it has been reported that the squeezing in the phase-dependent fluorescence spectra for two-level atoms in free space can also been found at a phase near $\pm 45°$ if the lifetime of the atoms is long when compared to the interaction time [10]. Zhao *et al* [24] have used a *thin-sample theory* to analyse the fluorescence squeezing spectra

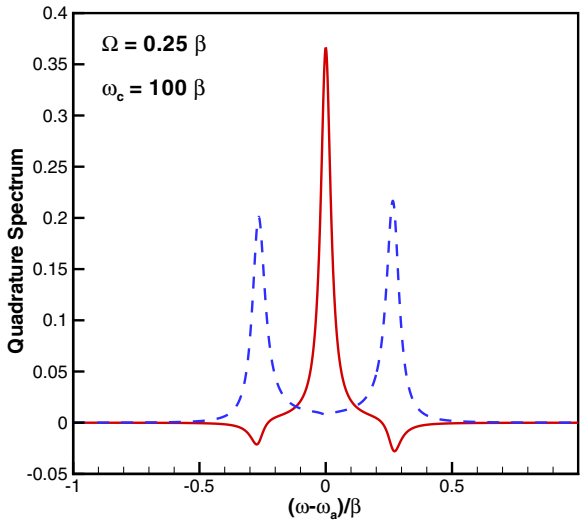

Figure 5. Resonance fluorescence quadrature spectra near the bandedge. Solid curve: in-phase, $S_1(\omega)$; dashed curve: out-of-phase, $S_2(\omega)$ with $\omega_c = 100\beta$ and $\Omega = 0.25\beta$.

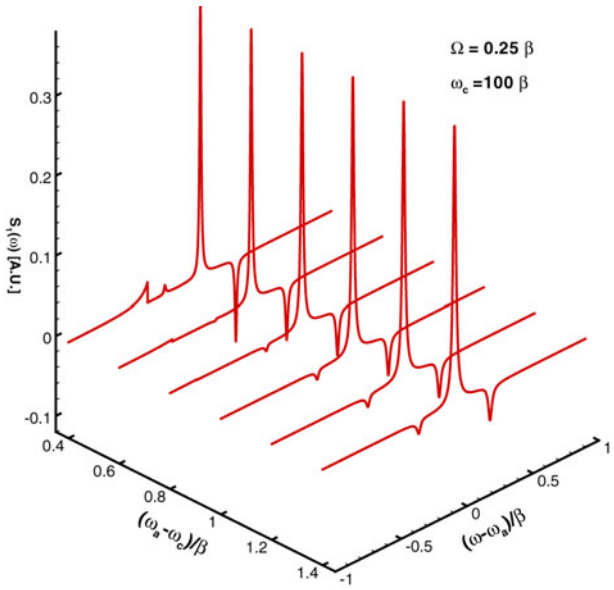

Figure 6. The evolution of in-phase quadrature spectra near the bandedge with $\omega_c = 100\beta$ and $\Omega = 0.25\beta$.

from the $^1S_0 \rightarrow {}^3P_1$ transition line of ^{174}Yb atoms, for which the lifetime is 875 ns.

The situations are different for the case of photonic bandgap crystals. When the transition frequency is near the bandedge of the photonic crystals, the bandgap effects modify the fluorescence intensity spectrum and cause asymmetric spectral profiles, as we have seen in figure 2. As shown in figure 5, for the case of photonic bandgap crystals, the in-phase quadrature not only contributes to the central component but also to the two sidebands. The out-of-phase quadrature still only contributes to the two sidebands as in the case of free space. Moreover, we find both sidebands of the in-phase quadrature now exhibit squeezing even when $\Omega^2 > 4\Gamma^2$. In the above calculation all the quadrature noise spectra are normalized with respect to the decay rate of the atom, Γ, as shown in equation (34). For the case of free space, the decay rate Γ is frequency independent due to the white noise reservoir. However, for photonic crystals, the decay rate will be modified according to the offset between the atomic transition frequency and the bandedge frequency. According to the works in [14, 18], the spontaneous emission rate of a two-level atom near the bandedge contains non-exponential terms. For simplicity we have used the following formula to estimate the decay rate of the atom:

$$\Gamma \approx \mathrm{Re}[\tilde{G}(\omega = 0)] = \beta^{3/2}\frac{\sqrt{\omega_a - \omega_c}}{\omega_a}. \qquad (35)$$

In figure 6, we plot the evolution of the in-phase quadrature spectra for different frequency (wavelength) offset. One can see that the higher frequency peak exhibits larger squeezing as well as larger fluorescence intensity when the offset frequency approaches the bandedge frequency.

In the literature, the in-phase quadrature squeezing of the resonance fluorescence from a laser-dressed two-level atom inside a cavity has been predicted based on the secular approximation [25]. Expressions for both the in-phase and out-of-phase quadrature spectra are derived and expressed in terms of the semiclassical density matrix elements under the dressed state picture. Qualitatively speaking, under the dressed state picture, they found that the Rabi sidebands will exhibit in-phase quadrature squeezing when ρ_{--} is somewhat larger than ρ_{++}, where ρ_{++} and ρ_{--} are the populations of the semiclassical dressed states $|+\rangle$ and $|-\rangle$. They also found that one can tune the cavity frequency as well as the driving laser frequency detuning to control the populations of the dressed states and produce squeezing or anti-squeezing in the in-phase quadrature. For our case of photonic bandgap crystals, the $|-\rangle \rightarrow |+\rangle$ transition (the lower frequency sideband) is suppressed when the atom is near the bandedge and the $|+\rangle \rightarrow |-\rangle$ transition (the higher frequency sideband) is enhanced. Intuitively this will also make the ρ_{--} larger than ρ_{++} and thus produce in-phase quadrature squeezing in both the Rabi sidebands. Of course the analyses in [25] cannot be directly applied to the case considered here. However, we believe that the physical mechanism of producing the in-phase quadrature squeezing should be similar. It will also be very interesting to carry out similar analyses based on the secular approximation for the case of photonic bandgap crystals in the future.

5. Conclusions

In conclusion, by introducing the Liouville operator expansion, we have successfully overcome some of the difficulties associated with the non-Markovian nature of the problem caused by the non-uniform distribution of the photon states in a photonic bandgap crystal. Our calculated results have indicated that the resonance fluorescence spectra near a photonic bandgap can exhibit interesting behaviour including the suppression and enhancement of the Mollow's triplet peaks, and the squeezing phenomena in the in-phase quadrature spectra. It will be very interesting to see if one can actually verify these predictions experimentally.

Acknowledgments

This work was supported in part by the National Science Council of the Republic of China under Grant No. NSC 92-2120-M-001-005, as well as by the Center for Nano-Science and Technology in the United System of Taiwan.

References

[1] Loudon R 1983 *The Quantum Theory of Light* 2nd edn (New York: Oxford University Press)
[2] Mollow R R 1969 *Phys. Rev.* **188** 1969
[3] Cohen-Tannoudji C 1977 *Frontiers in Laser Spectroscopy* ed R Balian, S Haroche and S Liberman (New York: North-Holland)
[4] Kimble H J, Dagenais M and Mandel L 1977 *Phys. Rev. Lett.* **39** 691
[5] Wu F Y, Ezekiel S, Ducloy M and Mollow B R 1977 *Phys. Rev. Lett.* **38** 1077
[6] Walls D F and Zoller P 1981 *Phys. Rev. Lett.* **47** 709
[7] Mandel L 1982 *Phys. Rev. Lett.* **49** 136
[8] Collett M J, Walls D F and Zoller P 1984 *Opt. Commun.* **52** 145
[9] Walls D F and Milburn G J 1984 *Quantum Optics* 2nd edn (Berlin: Springer)
[10] Lu Z H, Bali S and Thomas J E 1998 *Phys. Rev. Lett.* **81** 3635
[11] John S 1987 *Phys. Rev. Lett.* **58** 2486
[12] Yablonovitch E 1987 *Phys. Rev. Lett.* **58** 2059
[13] John S and Wang J 1990 *Phys. Rev. Lett.* **64** 2418
[14] John S and Quang T 1994 *Phys. Rev.* A **50** 1764
[15] Zhu S-Y, Chen H and Huang H 1997 *Phys. Rev. Lett.* **79** 205
[16] Paspalakis E and Knight P L 1998 *Phys. Rev. Lett.* **81** 293
[17] Paspalakis E, Kylstra N J and Knight P L 1999 *Phys. Rev.* A **60** R33
[18] Florescu M and John S 2001 *Phys. Rev.* A **64** 033801
[19] Lewenstein M, Zakrzewski J and Mossberg T W 1988 *Phys. Rev.* A **38** 808
[20] Purcell E M 1946 *Phys. Rev.* **69** 681
[21] Zhu S Y, Yang Y, Chen H, Zheng H and Zubairy M S 2000 *Phys. Rev. Lett.* **84** 2136
[22] Lewenstein M, Mossberg T W and Glauber R J 1987 *Phys. Rev. Lett.* **59** 775
[23] Yamamoto Y and İmamoğlu A 1999 *Mesoscopic Quantum Optics* (New York: Wiley)
[24] Zhao H Z, Lu Z H and Thomas J E 1997 *Phys. Rev. Lett.* **79** 613
[25] Zhou P and Swain S 1999 *Phys. Rev.* A **59** 1603